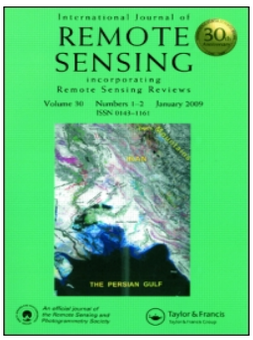

International Journal of Remote Sensing

ISSN: (Print) (Online) Journal homepage: https://www.tandfonline.com/loi/tres20

Evaluation of the version 5.0 global land surface satellite (GLASS) leaf area index product derived from MODIS data

Juan Li & Zhiqiang Xiao

To cite this article: Juan Li & Zhiqiang Xiao (2020) Evaluation of the version 5.0 global land surface satellite (GLASS) leaf area index product derived from MODIS data, International Journal of Remote Sensing, 41:23, 9140-9160, DOI: 10.1080/01431161.2020.1797222

To link to this article: https://doi.org/10.1080/01431161.2020.1797222

Published online: 03 Oct 2020.

INTERNATIONAL JOURNAL OF REMOTE SENSING
2020, VOL. 41, NO. 23, 9140–9160
https://doi.org/10.1080/01431161.2020.1797222

Evaluation of the version 5.0 global land surface satellite (GLASS) leaf area index product derived from MODIS data

Juan Li and Zhiqiang Xiao

State Key Laboratory of Remote Sensing Science, Faculty of Geographical Science, Beijing Normal University, Beijing, China

ABSTRACT

The Global Land Surface Satellite (GLASS) leaf area index (LAI) product is one of the most widely used global LAI products in the scientific community. The latest (version 5) GLASS LAI product has been generated from Moderate Resolution Imaging Spectroradiometer (MODIS) surface reflectance data. The purpose of this paper is to evaluate the quality of the version 5 GLASS LAI product. The GLASS LAI product was compared with the latest MODIS LAI product (MCD15A2 H, Collection 6) and the second version of Geoland2 (GEOV2) LAI product to evaluate their temporal and spatial discrepancies. A direct validation was conducted to compare these LAI products to the LAI values derived from the high-resolution reference maps from the Validation of Land European Remote Sensing Instruments (VALERI) and Implementing Multi-Scale Agricultural Indicators Exploiting Sentinels (IMAGINES) sites. The results show that the GLASS and GEOV2 LAI products have great spatial integrity. However, the MODIS LAI product contains many missing pixels in tropical areas. These LAI products follow fairly consistent seasonal characteristics. The spatial discrepancies of these LAI products mainly exist in forest areas, especially evergreen broadleaf forests where the GLASS LAI values are generally lower than the GEOV2 LAI values by approximately 1.0 LAI units and lower than the MODIS LAI values by 0.5 to 1.0 LAI units. The spatial distribution of these LAI products has slight discrepancies in savannahs, broadleaf crops, grasses/cereal crops and shrubs. The GLASS and GEOV2 LAI products capture a complete and reasonable temporal profile, contrasting with the MODIS LAI product, which shows dramatic fluctuations, particularly during the growing seasons. These LAI products show similar temporal trajectories and interannual variations for all biome types except evergreen broadleaf forests. The direct validation shows that the accuracy of the GLASS LAI product is better than the accuracy of the MODIS and GEOV2 LAI products. The coefficient of determination ($R2$) of the GLASS, MODIS and GEOV2 LAI products versus the LAI values derived from the high-resolution reference maps are 0.68, 0.47 and 0.55, respectively, and the root mean square error (RMSE) of these products are 0.86, 1.22 and 1.21, respectively.

ARTICLE HISTORY
Received 30 March 2020
Accepted 8 June 2020

CONTACT Zhiqiang Xiao zhqxiao@bnu.edu.cn State Key Laboratory of Remote Sensing Science, Faculty of Geographical Science, Beijing Normal University, Beijing 100875, China

1. Introduction

The leaf area index (LAI) is defined as half of the total green leaf area for a given unit of horizontal ground surface area (Chen and Black 1992). It is a critical structural parameter of the vegetation canopy. The traditional ground measurement method can obtain LAI data in only a small area. The development of remote sensing technology has realized the effective acquisition of long-time-series global LAI products. Existing major global LAI products include the first and second versions of Geoland2 (GEOV1/2) (Baret et al. 2013; Verger, Baret, and Weiss 2014), the Global Land Surface Satellite (GLASS) (Xiao et al. 2014, 2016a), the Moderate Resolution Imaging Spectroradiometer (MODIS) (Myneni et al. 2002), the third generation Global Inventory Monitoring and Modelling System (GIMMS3 g) (Zhu et al. 2013), the National Centres for Environmental Information (NCEI) (Claverie et al. 2016) and others.

Among these global LAI products, the GLASS LAI product has been widely used in the scientific community. Many researchers have used long-time-series GLASS LAI products to analyse the response of vegetation to the changing environment (Jiapaer et al. 2015). Zhu et al. (2016) investigated trends of the LAI and their drivers for the period from 1982 to 2009 using the GLASS LAI product and outputs from ecosystem models run at a global extent. The GLASS LAI product was used to evaluate land surface models (Bao et al. 2014; Druel et al. 2017; Guimberteau et al. 2018; Tesemma et al. 2015) and drought responses of Earth system models (Huang et al. 2016). The GLASS LAI product was also used to detect forest disturbances over the Daxinganling region of Northeast China and achieved good performance (Wang et al. 2017). In addition, the GLASS LAI product was used to calculate the fraction of absorbed photosynthetically active radiation (FAPAR) (Xiao et al. 2015, 2016b; Yan et al. 2016c), fractional vegetation cover (FVC) (Xiao et al. 2016c ; Song et al. 2017), broadband emissivity (BBE) over vegetated surfaces (Jie et al. 2016; Meng, Cheng, and Liang 2017), gross primary production (GPP) (Liu, Shao, and Liu 2015; Tian et al. 2017) and evapo-transpiration (ET) (Tian et al. 2015; Sun et al. 2016; Slessarev et al. 2016). Some researchers have used the GLASS LAI product as ancillary data to map wall-to-wall vegetation height data in China and improve the accuracy of estimated vegetation heights (Huang et al. 2017; Liu et al. 2016).

The current GLASS LAI product is widely used and is from the four versions. The spatial resolutions of the four versions of the GLASS LAI products are 5 km from Advanced Very High Resolution Radiometer (AVHRR) data and 1 km from MODIS data. To meet the requirements of various applications and provide users with higher quality products, the latest (version 5) GLASS LAI product has been generated. The version 5 GLASS LAI product, derived from MODIS surface reflectance data, has a spatial resolution of 500 m, a temporal resolution of eight days and spans from 2000 to 2018. Meanwhile, the version 6 MODIS LAI product was distributed by the National Aeronautics and Space Administration (NASA) at a spatial resolution of 500 m, and the latest GEOV2 LAI product was released by Europe.

It is vital to evaluate the accuracy of these latest global LAI products and understand the differences between these products for effective applications. Currently, many researchers have compared existing LAI products to analyse their discrepancies (Garrigues et al. 2008; Xiao, Liang, and Jiang 2017; Camacho et al. 2013; Jin et al. 2017). Xiao, Liang, and Jiang (2017) reported that the GLASS AVHRR and NCEI AVHRR LAI values

were in good agreement with the MODIS LAI values in tropical forests. However, the GLASS AVHRR and NCEI AVHRR LAI values were consistently lower than the Global Mapping (GLOBMAP) LAI values and higher than the GIMMS3 g LAI values in tropical forests. These LAI products were also directly validated using ground measurements (Garrigues et al. 2008; Fang, Wei, and Liang 2012) or lidar-based LAI values (Zhao and Popescu 2009). The Carbon cycle and Change in Land Observational Products from an Ensemble of Satellites (CYCLOPES) and Collection 4 MODIS LAI products were in better agreement with the ground-based measurements than was the GLOBCARBON LAI product over grasses and cereal crops (Garrigues et al. 2008). In addition, some studies have validated LAI products for a certain biome type (Fang et al. 2019; Claverie et al. 2013) or a certain area (Yang et al. 2017; Pisek and Chen 2007). Fang et al. (2019) examined seven global LAI products over croplands in north-eastern China and found that the uncertainties of these products over paddy rice fields were higher than those over other crop fields.

These validations are mainly aimed at the versions 4 and 5 MODIS products, CYCLOPES, GEOV1, GIMMS3 g, and NCEI. There is little evaluation of the version 6 MODIS LAI product and the GEOV2 LAI product, and the 500 m GLASS LAI product has not been validated. In this study, these LAI products are compared to evaluate their temporal and spatial consistencies and continuities. At the same time, these LAI products are compared with the LAI values derived from the high-resolution reference maps to evaluate their accuracy.

This paper is organized as follows. The second section of this paper provides an introduction of the GLASS, MODIS and GEOV2 LAI products and the high-resolution LAI reference maps used in this paper. Section 3 describes the approaches used for evaluating the LAI products. The spatiotemporal consistency analyses among these LAI products and a comparison of these LAI products with the LAI values derived from high-resolution reference maps are presented in Section 4. Our conclusions are drawn in the last section.

2. Data

2.1. Global LAI products

2.1.1. GLASS LAI product

The GLASS LAI product offers a temporal resolution of 8 days. It includes two datasets, GLASS AVHRR and GLASS MODIS (Xiao et al. 2016a). The GLASS AVHRR LAI product was produced from the version 4 Long-Term Data Record (LTDR) AVHRR surface reflectance data. It is provided in a geographic latitude/longitude projection at a spatial resolution of 0.05° (approximately 5 km at the equator) and spans from 1981 to 2018. The GLASS MODIS LAI product was produced from the MODIS surface reflectance product (MOD09A1) and is provided in a sinusoidal projection. The version 4 GLASS MODIS LAI product was generated from the collection 5 MODIS surface reflectance product. It has a 1 km spatial resolution and spans from 2000 to 2015. The latest (version 5) GLASS MODIS LAI product was generated from the collection 6 MODIS surface reflectance product. This product has a spatial resolution of 500 m and spans the period from 2000 to 2018.

The retrieval algorithm of the GLASS MODIS LAI product uses general regression neural networks (GRNNs) with multiple inputs and outputs. Time-series fused LAI values from the MODIS and CYCLOPES LAI products and the corresponding pre-processed MODIS surface reflectance data of the Benchmark Land Multisite Analysis and Inter-comparison of

Products (BELMANIP) sites were used to train the GRNNs (Xiao et al. 2014). The pre-processed MODIS reflectance data from an entire year were inputted to the GRNNs to estimate the one year LAI profiles. The performance of the GLASS MODIS LAI product from the latest version was evaluated in this study.

2.1.2. MODIS LAI product

The latest version of the MODIS LAI product is Collection 6. The Collection 6 combined MODIS LAI product has two datasets at a spatial resolution of 500 m, MCD15A2 H and MCD15A3 H. The MCD15A2 H LAI product has a temporal resolution of 8 days, while the MCD15A3 H LAI product has a temporal resolution of 4 days. In this study, the MCD15A2 H LAI product is used for comparative analysis. The MCD15A2 H product has been available since 2002 and is provided in a sinusoidal projection.

The MODIS LAI retrieval algorithm is composed of a main algorithm and a backup algorithm (Yan et al. 2016a). The main algorithm is based on look-up tables constructed by a three-dimensional radiative-transfer model. The input data of the main algorithm are MODIS surface reflectance data and a biome map. The backup algorithm is used only when the main algorithm fails to estimate LAI values. The backup algorithm is based on biome-specific LAI-Normalized Difference Vegetation Index (NDVI) relationships and estimates LAI values with comparatively poor quality (Yang et al. 2006).

2.1.3. GEOV2 LAI product

The GEOV2 LAI product is the second version of biophysical products under the Geoland2 project. It is provided in a Plate-Carrée projection at a spatial resolution of 1/112° (approximately 1 km at the equator) and a temporal resolution of 10 days. The GEOV2 LAI product was available from 1999 to the present. Before 2014, the GEOV2 LAI product was generated from the Systeme Probatoire d'Observation de la Terre (SPOT)-VEGETATION data, and the GEOV2 LAI product from 2014 to the present was generated from Project for On-Board Autonomy-Vegetation (PROBA-V) surface reflectance data.

The retrieval algorithm of GEOV2 LAI is a neural network that was trained by fused LAI values from Collection 5 MODIS and CYCLOPES LAI products and the surface reflectance of SPOT-VEGETATION and PROBA-V over the global BELMANIP sites (Baret et al. 2013). The multistep filtering method is used to eliminate LAI values contaminated by atmospheric effects and snow cover (Verger, Baret, and Weiss 2013).

2.2. Field measurements

In this paper, 58 high-resolution LAI reference maps provided by 38 sites of the Validation of Land European Remote Sensing Instrument (VALERI) and Implementing Multi-Scale Agricultural Indicators Exploiting Sentinels (IMAGINES) projects were collected to validate the GLASS, MODIS and GEOV2 LAI products.

To validate biophysical parameter products obtained from satellite data, the VALERI and IMAGINES projects used a LAI-2000 Plant Canopy Analyser and hemispheric photography to obtain LAI ground measurements. A transfer function between the reflectance values of the high-spatial-resolution satellite images, SPOT or Land Remote-Sensing Satellite System-8 (LANDSAT-8), and the LAI ground measurements is utilized to scale-up ground measurement data and generate LAI reference maps (Camacho et al. 2013).

The time span of the LAI ground measurements of the VALERI project is from 2000 to 2008 and that of the IMAGINES project is from 2013 to 2016.

The high-resolution LAI reference maps were aggregated over an area of 1 km × 1 km, which contains approximately 4 GLASS or MODIS pixels and 1 GEOV2 pixel. The characteristics and average LAI values of the selected sites are shown in Table 1. At these sites, there are eight biome types according to the MODIS land-cover type product (MCD12Q1). The eight biome types are savannahs, broadleaf crops, grasses and cereal crops, shrubs, evergreen broadleaf forests, deciduous broadleaf forests, evergreen needleleaf forests and deciduous needleleaf forests.

3. Methodology

To evaluate the performance of the latest GLASS LAI product, the inter-comparison with the MODIS and GEOV2 LAI products and direct validation with ground measurements were performed in this study.

For comparisons of spatial consistency, the global maps of these LAI products in January and July 2013 and the histograms of these LAI products for July 2013 in the Northern and Southern Hemispheres were computed to analyse the distribution of each product. The histogram distributions of these LAI products for each biome type according to the MODIS land-cover type product in July 2013 were used to investigate similarities and differences of these LAI products. Furthermore, the differences between GLASS and the other two LAI products in July 2013 and their histogram distributions were generated to evaluate the spatial consistency among these products. Only the pixels with LAI values in all three LAI products were used to create histograms.

Africa, which is divided by the equator, has a special geographic position and rich vegetation types. In this paper, the African continent was selected to evaluate the consistency of these products at the regional scale. In the same way as Yan et al. (2016b) and Garrigues et al. (2008), profiles of mean LAI values from these products in a region with width of 20 km along 25° E over Africa were compared in January and July 2013.

To evaluate their temporal consistencies, the temporal profiles of the GLASS, MODIS and GEOV2 LAI products were checked over a selection of sites (Table 1) with different biome types. For each site, the LAI profiles from 2002 to 2018 were compared to provide a qualitative analysis of seasonal variations and temporal consistencies among these LAI products.

Subsequently, the GLASS, MODIS and GEOV2 LAI values were validated against 58 LAI values derived from the high-resolution reference maps. The discrepancies of each product were quantified by the regression equation, coefficient of determination ($R2$) and root mean square error (RMSE).

The GLASS, MODIS and GEOV2 LAI products have different projections and spatiotemporal resolutions. For evaluations of their spatiotemporal consistency, the projections of the GLASS and MODIS products were transformed into Plate-Carrée projection, and these two LAI products were resampled to a 1 km spatial resolution by the nearest neighbour resampling method. All LAI products were aggregated into a monthly time step using the averaging method. The pixel values, which are available for at least 75% of a month, will be used for the computation. However, any reprojection and resampling would increase

Table 1. Characteristics of the 38 selected sites and their mean LAI values.

Site name	Country	Latitude (°)	Longitude (°)	Biome type	Year	Day of year	Mean LAI
Alpilles	France	43.81	4.71	Grasses/cereal crops	2002	204	1.79
Camerons	Australia	−32.60	116.25	Savanna	2004	63	2.34
Counami	French Guyana	5.34	−53.24	Evergreen broadleaf forest	2002	286	4.38
Demmin	Germany	53.89	13.21	Broadleaf crop	2004	164	4.55
Donga	Benin	9.77	1.78	Savanna	2005	172	1.81
Gilching	Germany	48.08	11.32	Grasses/cereal crops	2002	199	4.99
Gnangara	Australia	−31.53	115.88	Savanna	2004	61	1.05
Laprida	Argentina	−36.99	−60.55	Broadleaf crop	2002	292	2.77
Larose	Canada	45.38	−75.22	Savanna	2003	219	5.82
Larzac	France	43.94	3.12	Savanna	2002	183	0.71
Plan-de-Dieu	France	44.20	4.95	Grasses/cereal crops	2004	189	1.09
Sonian	Belgium	50.77	4.41	Deciduous broadleaf forest	2004	174	5.69
Sud_Ouest	France	43.51	1.24	Broadleaf crop	2002	189	2.05
Turco	Bolivia	−18.24	−68.18	Shrub	2002	240	0.04
Zhangbei	China	41.28	114.69	Grasses/cereal crops	2002	221	1.34
Pshenichne	Ukraine	50.08	30.23	Grasses/cereal crops	2013	134	0.32
Pshenichne	Ukraine	50.08	30.23	Grasses/cereal crops	2013	166	2.09
Pshenichne	Ukraine	50.08	30.23	Grasses/cereal crops	2013	196	3.61
SouthWest_1	France	43.55	1.09	Grasses/cereal crops	2013	173	1.44
SouthWest_1	France	43.55	1.09	Grasses/cereal crops	2013	191	0.92
SouthWest_1	France	43.55	1.09	Grasses/cereal crops	2013	207	1.06
SouthWest_1	France	43.55	1.09	Grasses/cereal crops	2013	230	1.72
SouthWest_1	France	43.55	1.09	Grasses/cereal crops	2013	247	1.19
SouthWest_2	France	43.45	1.15	Grasses/cereal crops	2013	173	1.34
SouthWest_2	France	43.45	1.15	Grasses/cereal crops	2013	191	0.58
SouthWest_2	France	43.45	1.15	Grasses/cereal crops	2013	207	0.38
SouthWest_2	France	43.45	1.15	Grasses/cereal crops	2013	230	2.04
SouthWest_2	France	43.45	1.15	Grasses/cereal crops	2013	247	1.78
25de Mayo_Alfalfa	Argentina	−37.91	−67.75	Grasses/cereal crops	2014	40	2.27
25de Mayo_Shurb	Argentina	−37.94	−67.79	Shrub	2014	40	0.17
Rosasco	Italy	45.25	8.56	Grasses/cereal crops	2014	184	4.18
LaReina_Cordoba_1	Spain	37.82	−4.86	Grasses/cereal crops	2014	140	1.31
LaReina_Cordoba_2	Spain	37.79	−4.83	Grasses/cereal crops	2014	140	2.23
Barrax-LasTiesas	Spain	39.05	−2.10	Broadleaf crop	2014	149	0.86
Albufera	Spain	39.27	−0.32	Evergreen needleleaf forest	2014	158	0.46
Albufera	Spain	39.27	−0.32	Evergreen needleleaf forest	2014	175	1.38
Albufera	Spain	39.27	−0.32	Evergreen needleleaf forest	2014	196	3.66
Albufera	Spain	39.27	−0.32	Evergreen needleleaf forest	2014	219	5.66
Albufera	Spain	39.27	−0.32	Evergreen needleleaf forest	2014	234	5.81
Pshenichne	Ukraine	50.08	30.23	Grasses/cereal crops	2014	163	1.58
Pshenichne	Ukraine	50.08	30.23	Grasses/cereal crops	2014	212	2.39
Capitanata	Italy	41.46	15.49	Grasses/cereal crops	2014	77	2.56
Capitanata	Italy	41.46	15.49	Grasses/cereal crops	2014	133	3.31
SanFernando	Chile	−34.72	−71.00	Grasses/cereal crops	2015	19	1.99
Barrax-LasTiesas	Spain	39.05	−2.10	Broadleaf crop	2015	145	2.24
Barrax-LasTiesas	Spain	39.05	−2.10	Broadleaf crop	2015	203	0.68
Pshenichne	Ukraine	50.08	30.23	Grasses/cereal crops	2015	174	2.27
Pshenichne	Ukraine	50.08	30.23	Grasses/cereal crops	2015	188	2.42
Pshenichne	Ukraine	50.08	30.23	Grasses/cereal crops	2015	204	3.02
Peyrousse	France	43.67	0.22	Grasses/cereal crops	2015	174	0.73
Urgons	France	43.64	−0.43	Broadleaf crop	2015	174	2.07
Creón D'armagnac	France	43.99	−0.05	Evergreen broadleaf forest	2015	175	2.18

(*Continued*)

Table 1. (Continued).

Site name	Country	Latitude (°)	Longitude (°)	Biome type	Year	Day of year	Mean LAI
Condom	France	43.97	0.34	Grasses/cereal crops	2015	176	1.17
Savenès	France	43.82	1.17	Grasses/cereal crops	2015	176	0.97
Collelongo	Italy	41.85	13.59	Deciduous broadleaf forest	2015	189	4.89
Collelongo	Italy	41.85	13.59	Deciduous broadleaf forest	2015	266	3.94
Capitanata	Italy	41.46	15.49	Grasses/cereal crops	2015	113	2.98
Maragua_UpperTana	Kenya	−0.77	36.97	Grasses/cereal crops	2016	68	1.58

additional uncertainties in the LAI products. Thus, for direct validation, the original projection and spatial resolution of these LAI products were maintained, and projections of the high-resolution reference maps were converted to the corresponding projections of these LAI products. The GLASS and MODIS LAI values with a spatial resolution of 500 m at each site were aggregated over a 1 km × 1 km area by the averaging method, and the LAI reference maps for each site were scaled up to a 1 km spatial resolution in the corresponding projection of the LAI products. Differences in time between the LAI reference maps and LAI products were observed. LAI products adjacent to the time of ground measurement were processed by the linear interpolation method to obtain the LAI values with the same time as the ground measurements in this study.

Since the quality of the MODIS LAI values retrieved by the backup algorithm is poor, only the MODIS LAI values retrieved by the main algorithm were used in our performance evaluation except the spatial integrity comparison of the MODIS LAI product.

4. Results

4.1. Spatial consistency

The spatial distributions of the GLASS, MODIS and GEOV2 LAI products at the global scale in January and July 2013 are shown in Figure 1. Areas masked in white correspond to pixels in which the LAI values were missing or there was no vegetation. The MODIS LAI product contains a large number of missing pixels around the equator. This pattern is due to cloud contamination and poor atmospheric conditions. However, the GLASS and GEOV2 LAI products have better spatial integrity. The spatial integrity of the GLASS LAI product can be attributed to the GLASS LAI retrieval algorithm, which uses the pre-processed MODIS reflectance data from an entire year as its input to estimate one year LAI profiles for each pixel (Xiao et al. 2016a). The GEOV2 product uses a gap-filling climatic approach to ensure spatial integrity. The GEOV2 LAI values are missing only if the climatology is not available because of large discontinuities in the climatological data (Verger, Baret, and Weiss 2013).

Figure 1 demonstrates that these LAI products follow the seasonality effect, which shows opposite characteristics in the Northern and Southern Hemispheres. In the Northern Hemisphere, the LAI values in January are universally lower than those in July, and the spatial variation in the LAI values in January is obviously smaller than that in July. The LAI values of the middle-high latitudes in the Northern Hemisphere in July are relatively larger than those in January. The spatial distribution differences among the

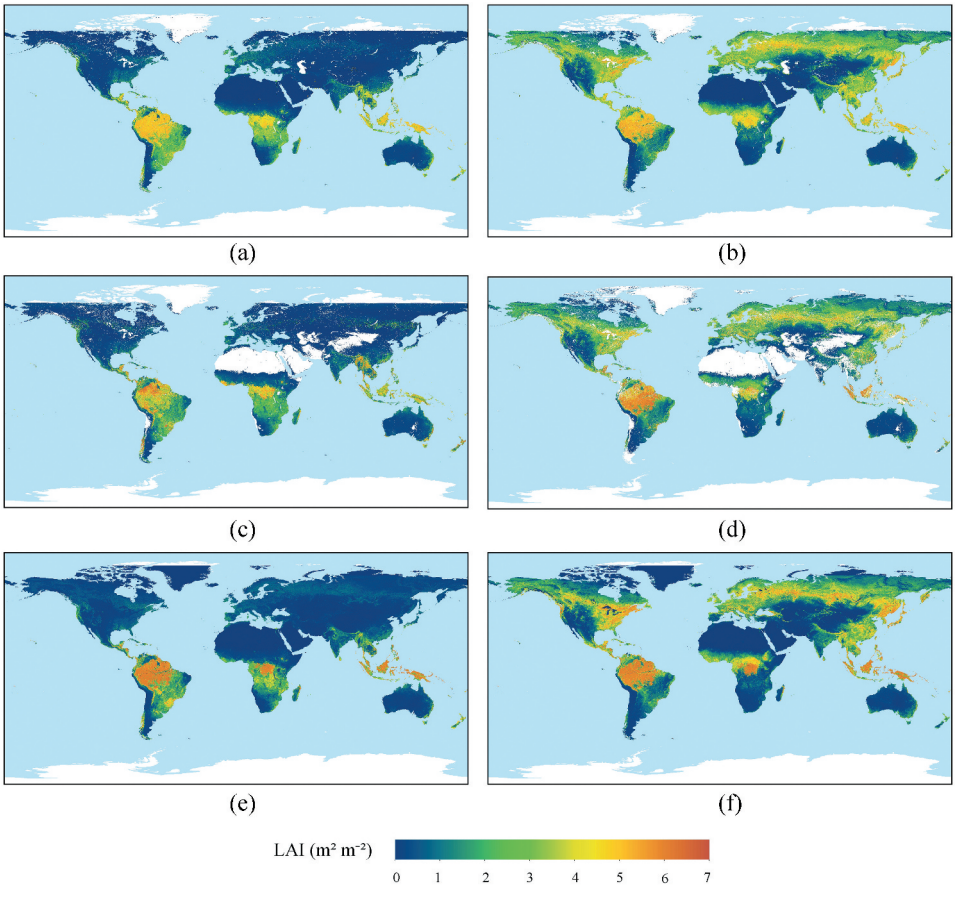

Figure 1. Global spatial distributions of the GLASS, MODIS and GEOV2 LAI products in January and July 2013. (a) GLASS LAI, January 2013. (b) GLASS LAI, July 2013. (c) MODIS LAI, January 2013. (d) MODIS LAI, July 2013. (e) GEOV2 LAI, January 2013. (f) GEOV2 LAI, July 2013.

three LAI products are mainly reflected in tropical rainforests. The GEOV2 LAI product has a relatively higher value in tropical rainforest than those of the GLASS and MODIS LAI products. Furthermore, the high LAI values are concentrated in the tropical rainforest near the equator, and the low LAI values are concentrated in areas with sparse vegetation.

Figure 2 displays the transects of the mean LAI values from these LAI products in a region with a width of 20 km along 25° E over Africa in January and July 2013. There are obvious differences among the GLASS, MODIS and GEOV2 LAI products in the vicinity of the equator in January and July 2013. The difference in the transects of these LAI products in January is greater than that in July over southern Africa. However, a similar trend of transects of the GLASS and GEOV2 LAI values in January and July can be seen with latitude, despite the LAI values being different.

For transects of the GLASS, MODIS and GEOV2 LAI products over Africa in January 2013, obvious differences among these LAI products can be captured in tropical African forests, tropical wooded grasslands and subtropical wooded grasslands. For tropical African forests, the values of the GEOV2 LAI product are significantly higher than the GLASS LAI

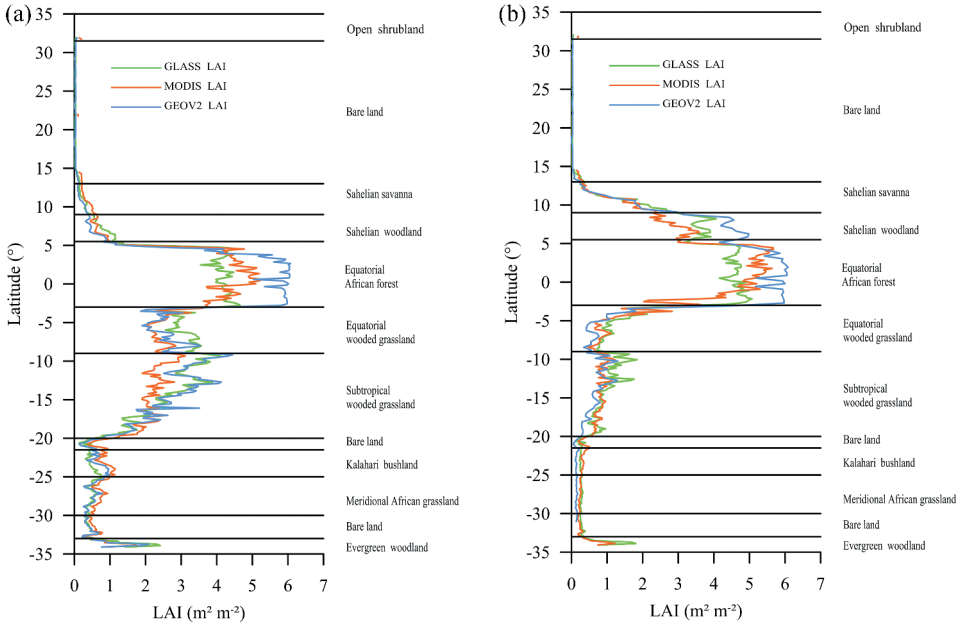

Figure 2. Transects of the GLASS, MODIS and GEOV2 LAI products over Africa for (a) January and (b) July 2013.

values, and the maximum difference is greater than 2 LAI units. For subtropical wooded grassland, the transect of the GLASS LAI product excellently agrees with that of the GEOV2 LAI product. The values of the GLASS and GEOV2 LAI products are higher than the MODIS LAI values, and the maximum difference is greater than 1.0 LAI unit. In contrast, these LAI products have a relatively small difference in tropical wooded grassland, and the maximum difference is less than 1.0 LAI unit.

For transects of these LAI products over Africa in July 2013, apparent differences among these LAI products can be observed in tropical African forests and Saharan woodlands. The values of the GEOV2 and MODIS LAI are higher than the GLASS LAI values in tropical African forests, among which the GEOV2 LAI values are generally the highest. The maximum difference between the GEOV2 LAI values and the GLASS LAI values is approximately 1.3 LAI units in tropical African forest. The GLASS LAI values are higher than the MODIS LAI values and lower than the GEOV2 LAI values in Saharan woodland. These products agree better over savannahs. In the African grassland, the GLASS and MODIS LAI values have a good consistency, but the GEOV2 LAI values are relatively low. These analyses may further confirm that the GEOV2 LAI values are higher than the GLASS and MODIS LAI values in tropical forests.

Histograms of the GLASS, MODIS and GEOV2 LAI values for July 2013 in the Northern and Southern Hemispheres are shown in Figure 3. When LAI values are less than 1.2 LAI units, the histograms of the GLASS, MODIS and GEOV2 LAI values in the Northern Hemisphere are significantly lower than those in the Southern Hemisphere. In contrast, the histograms of the GLASS, MODIS and GEOV2 LAI values between 1.2 and 5.0 LAI units in the Northern Hemisphere are significantly higher than those in the Southern Hemisphere. This result is consistent with the seasonal characteristics of vegetation

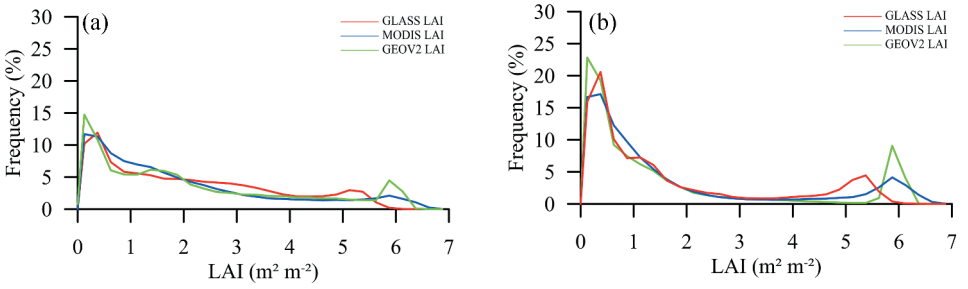

Figure 3. Histogram distributions of the GLASS, MODIS and GEOV2 LAI products for July 2013 in the (a) Northern and (b) Southern Hemispheres.

growth in the two hemispheres. For frequency distributions in the Southern Hemisphere, the histograms of the MODIS and GEOV2 LAI values have one similar peak near 5.9, and the histogram of the GLASS LAI values has one peak near 5.3. The peak of the GEOV2 LAI frequency distribution in the Southern Hemisphere is obviously higher than that of the other LAI products. However, these phenomena could not be observed in the histograms of these LAI products in the Northern Hemisphere. These results are partly due to the overestimation of the MODIS LAI product for the broadleaf forest (Garrigues et al. 2008) and the GEOV2 LAI values in the tropical rainforests are higher than the GLASS and MODIS LAI values. The highest LAI value of the GLASS LAI product reached 6.0, and the highest LAI value of the GEOV2 LAI product was below 6.5. Nevertheless, the highest LAI value of the MODIS LAI product exceeds 6.5. This result indicates that the MODIS LAI product has the largest dynamic range of LAI to depict the global variability of LAI.

Histograms of the GLASS, MODIS and GEOV2 LAI products in July 2013 for each biome type according to the MODIS land cover product are shown in Figure 4. The frequency distributions of all LAI products have a good consistency for grasses/cereal crops and shrubs. The frequency peak positions of the GLASS and MODIS LAI values are equal (approximately 0.5) and slightly higher than that of the GEOV2 LAI values in grasses/cereal crops. For broadleaf crops, the frequency distributions of these LAI products are quite different. The frequency distributions of the GLASS and GEOV2 LAI products have two peaks and that of the MODIS LAI product has only one peak. However, the first peak position of the GLASS LAI frequency distribution agrees with that of the MODIS LAI frequency distribution, and the two peak positions of the GLASS LAI frequency distribution are larger than the corresponding peak positions of the GEOV2 LAI frequency distribution. When the LAI value is less than 0.5 LAI units, the frequency distribution of the MODIS LAI product is in good agreement with that of the GEOV2 LAI product, and the frequency values of the MODIS and GEOV2 LAI products are slightly higher than that of the GLASS LAI product. However, the frequency of the GLASS LAI values between 2.2 and 3.5 LAI units is higher than that of the MODIS and GEOV2 LAI values. For savannahs, the frequency of the MODIS LAI values is higher than that of the GLASS LAI values when the LAI value between 1.0 and 2.0 LAI units. The peak position of the GLASS LAI frequency distribution is slightly higher than those of the MODIS and GEOV2 LAI frequency distributions. For the evergreen broadleaf forests, the three LAI products all display frequency distributions with a narrow peak.

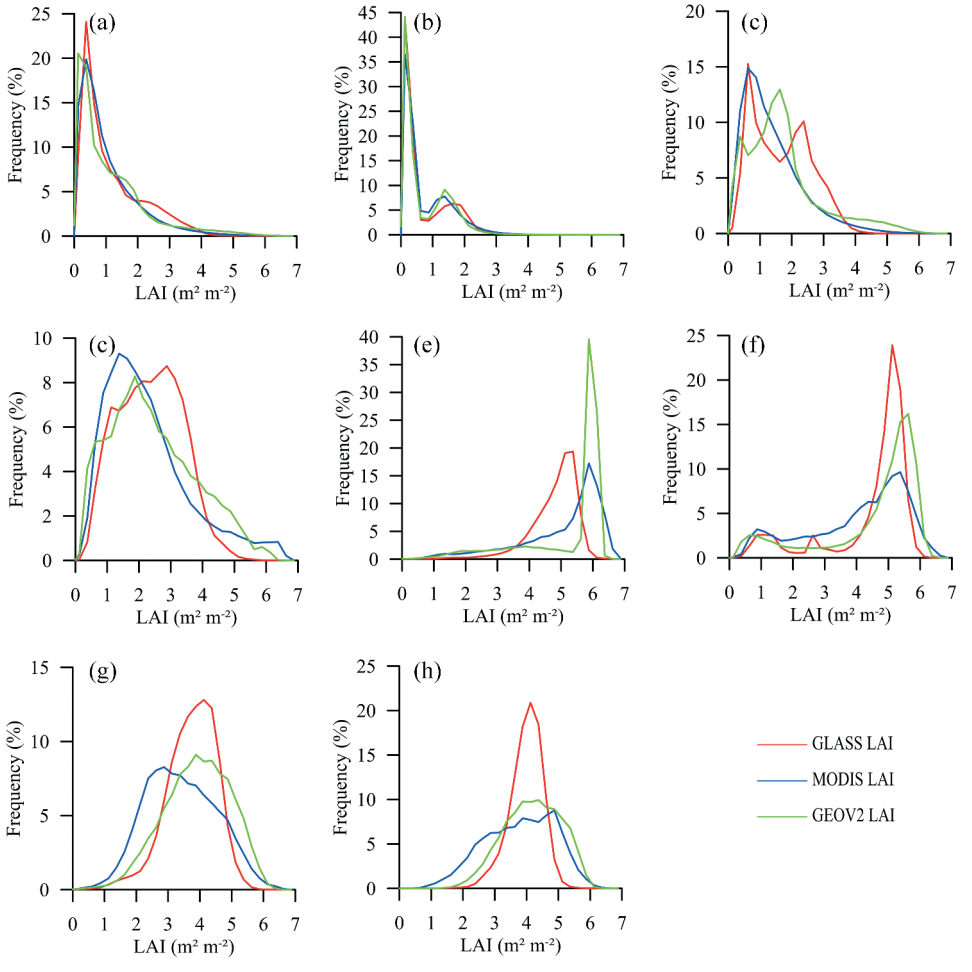

Figure 4. Histograms of the GLASS, MODIS and GEOV2 LAI products in July 2013 for different biome types. (a) Grasses and cereal crops. (b) Shrubs. (c) Broadleaf crops. (d) Savannahs. (e) Evergreen broadleaf forests. (f) Evergreen needleleaf forests. (g) Deciduous broadleaf forests. (h) Deciduous needleleaf forests.

The peak positions of the MODIS LAI and GEOV2 LAI frequency distributions are all approximately 5.9 LAI units, while that of the GLASS LAI is 5.3 LAI units, and the peak of the GEOV2 LAI frequency distribution is higher than that of the MODIS and GLASS LAI products. This result indicates that the GEOV2 LAI values are obviously larger than those of the other LAI products in evergreen broadleaf forests. For other forest biome types, the peak of the GLASS LAI frequency distribution is higher than that of the other LAI products, indicating that the GLASS LAI product is more concentrated in these biome types. For the evergreen coniferous forests, the frequency distributions of these LAI products show a degree of agreement, although the peak positions of these frequency distributions are slightly different. For deciduous broadleaf forests and deciduous needleleaf forests, the frequency of the MODIS LAI values less than 3.0 LAI units is larger than that of the GLASS and GEOV2 LAI values, while the frequency

of the GEOV2 LAI values greater than 5.0 LAI units is larger than that of the GLASS and MODIS LAI values. Therefore, differences in the GLASS, MODIS and GEOV2 LAI products are mainly in forest biome types. For forests, the frequency of the GEOV2 LAI high values is significantly higher than that of the GLASS and MODIS LAI values, particularly for evergreen broadleaf forests. The frequency of the MODIS LAI low values is significantly higher than that of the GLASS and GEOV2 LAI values.

Global maps of differences between the GLASS and the GEOV2 and MODIS LAI products in July 2013 are shown in Figure 5. Differences were calculated by the GLASS LAI values minus the MODIS or GEOV2 LAI values. It can be seen that the spatial distribution differences among these LAI products mainly occur in tropical rainforests and middle-high latitudes of the Northern Hemisphere, where the GLASS LAI values are generally lower than the GEOV2 LAI values of approximately 1.0 LAI units and lower than the MODIS LAI values between 0.5 and 1.0 LAI units.

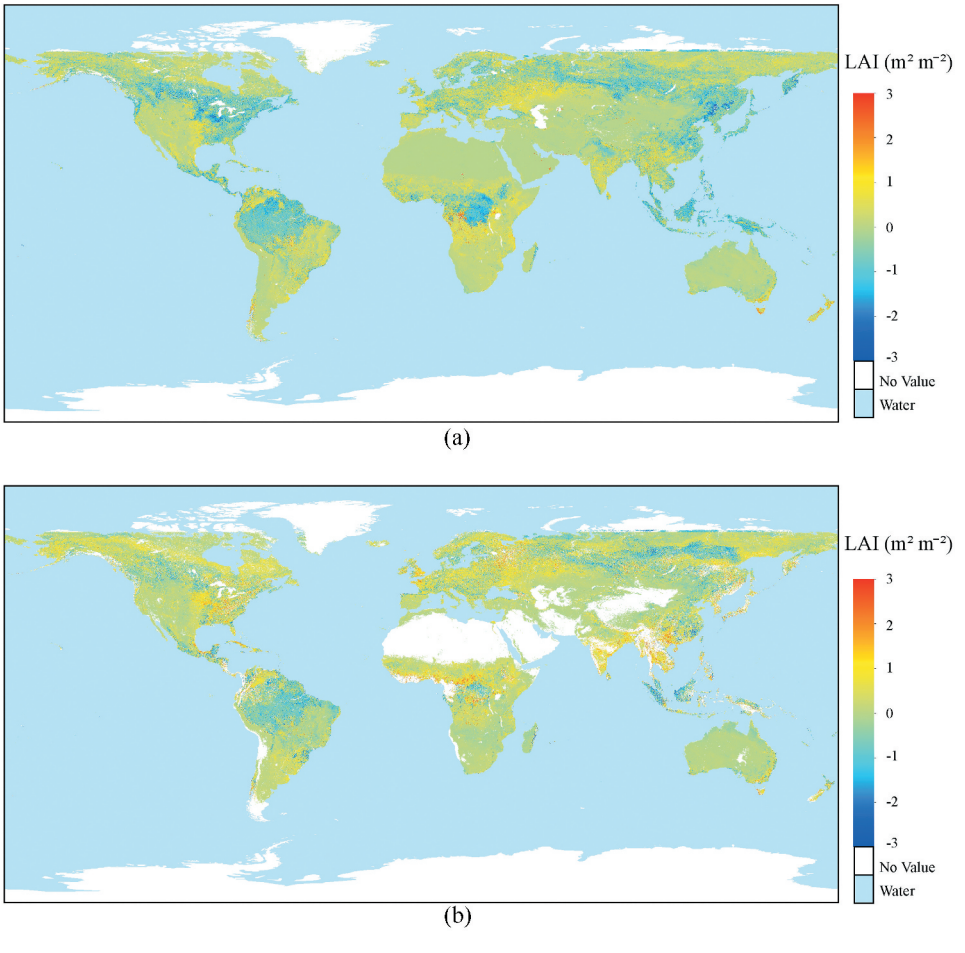

Figure 5. Spatial distributions of differences between the GLASS LAI product and the GEOV2 and MODIS LAI products in July 2013. (a) GLASS LAI minus GEOV2 LAI. (b) GLASS LAI minus MODIS LAI.

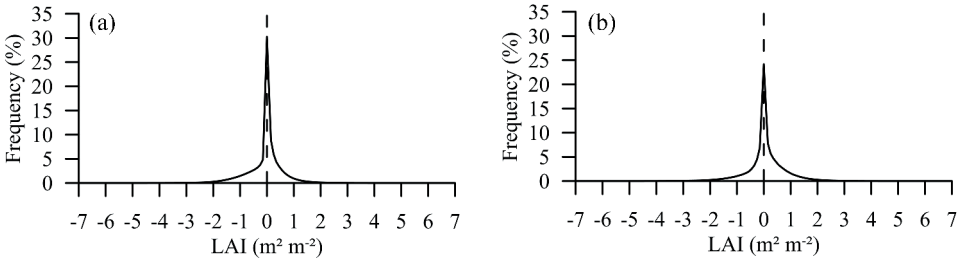

Figure 6. Histograms of differences (a) between the GLASS and GEOV2 LAI products, and (b) between the GLASS and MODIS LAI products in July 2013.

Figure 6(a) shows the histogram of differences between the GLASS and GEOV2 LAI products. Differences are concentrated around zero, for which the frequency is higher than 30%. The percentage of differences between −0.5 and 0.5 reaches 67.47%.

Figure 6(b) shows the histogram of differences between the GLASS and MODIS LAI products. Differences are also concentrated at zero. The percentage of differences at the zero value is 24.18%, and 63.69% of pixels are between −0.5 and 0.5. The spatial variation between the GLASS LAI product and the MODIS LAI product is slightly larger than that between the GLASS LAI product and the GEOV2 LAI product. Comparing histograms of differences between the GLASS and the GEOV2 and MODIS LAI products, it can be found that when differences are between 1.0 and 2.0 LAI units, the histogram of differences between the GLASS and MODIS LAI products has a higher frequency than that of differences between the GLASS and GEOV2 LAI products. This result may be partly due to the pixel value of the MODIS LAI product, which is influenced by clouds, atmosphere and other factors and is obviously smaller than that of the corresponding GEOV2 LAI product.

4.2. Temporal consistency

Thirteen sites with different biome types (shown in Table 1) were selected to analyse the temporal consistency of the GLASS, MODIS and GEOV2 LAI products from 2002 to 2018.

Figure 7(a, b) shows the temporal LAI trajectories at the Camerons and Larose sites form 2002 to 2018, respectively. The biome type of these sites is savannahs according to the MODIS land-cover type product. At the Camerons site, these LAI products show similar temporal trajectories and seasonal variations. The GEOV2 LAI values are generally greater than the MODIS LAI values for these years. The GLASS LAI values are between the GEOV2 and MODIS LAI values. Before 2004 and after 2009, the GLASS LAI values are in good agreement with the GEOV2 LAI values. However, from 2004 to 2009, the GLASS LAI values are in good agreement with the MODIS LAI values. The GLASS LAI values are closer to the LAI value derived from the high-resolution reference map than the MODIS and GEOV2 LAI values. At the Larose site, the temporal profiles of the GLASS and GEOV2 LAI products are smooth. However, during the growing seasons, the temporal profile of the MODIS LAI product is very noisy, with sudden peak and valley values. The GLASS, MODIS and GEOV2 LAI products capture similar seasonal characteristics and interannual variations. The

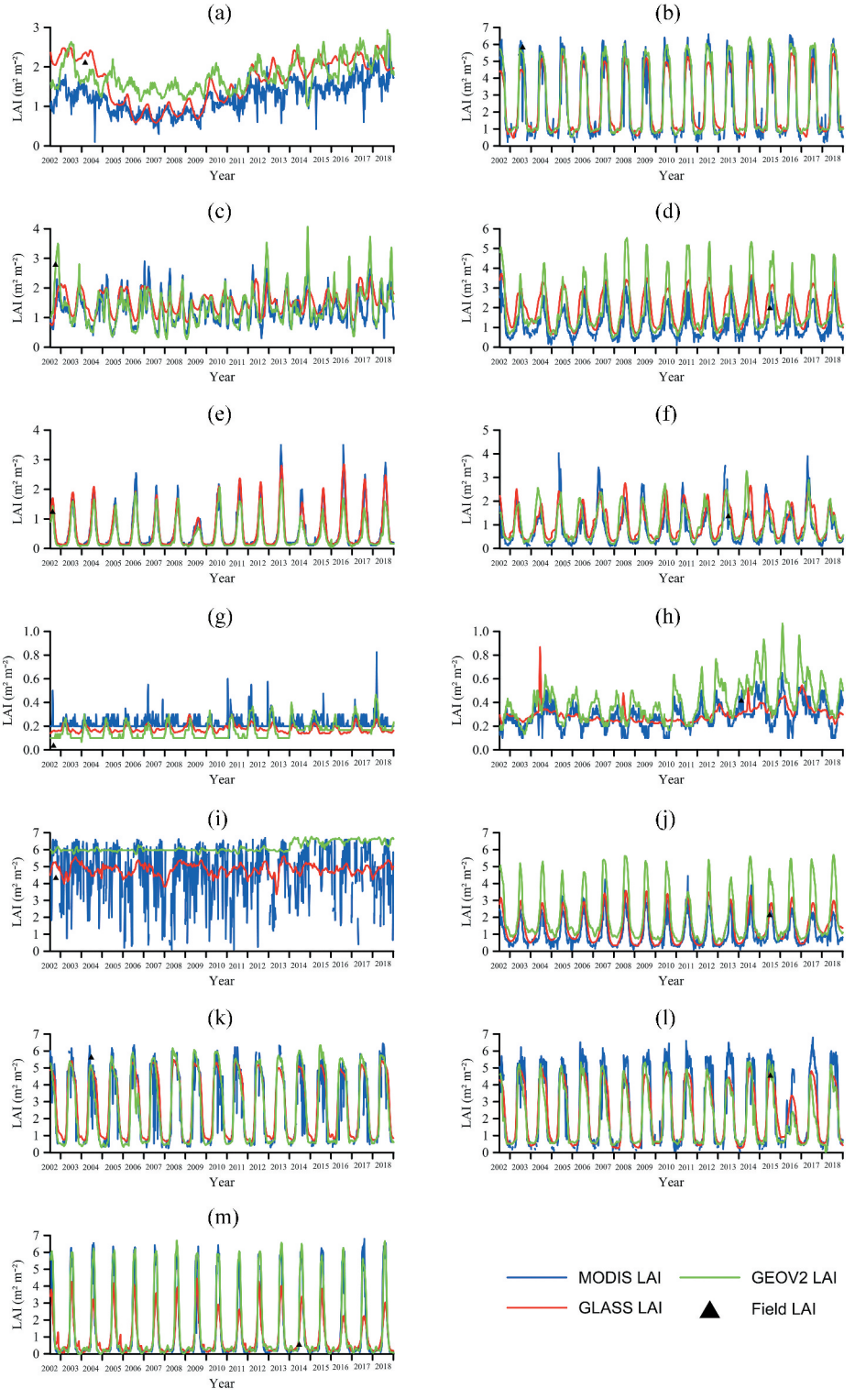

Figure 7. Temporal profiles of the GLASS, MODIS and GEOV2 LAI products over thirteen sites with different biome types. (a) Camerons. (b) Larose. (c) Laprida. (d) Urgons. (e) Zhangbei. (f) SouthWest_1. (g) Turco. (h) Mayo. (i) Counami. (j) Creón D'armagnac. (k) Sonian. (l) Collelongo. (m) Albufera.

GLASS, MODIS and GEOV2 LAI values are in good agreement during the non-growing seasons. However, during the growing seasons, the MODIS and GEOV2 LAI values are larger than the GLASS LAI values.

Figure 7(c, d) expresses the LAI temporal profiles at the Laprida and Urgons sites with broadleaf crops, respectively. For the Laprida site, the GLASS LAI values are generally greater than the MODIS and GEOV2 LAI values during the non-growing seasons. However, the MODIS and GEOV2 LAI values are generally greater than the GLASS LAI values during the growing seasons. Over the Urgons site, a good temporal consistency is achieved among the GLASS, MODIS and GEOV2 LAI values during the non-growing seasons. However, the GEOV2 LAI values are generally larger than the GLASS and MODIS LAI values during the growing seasons. The MODIS and GEOV2 LAI values are closer to the LAI value derived from the high-resolution reference map than the GLASS LAI values at the Urgons sites.

Over grass and cereal crop sites, the temporal LAI trajectories are presented in Figure 7(e, f). It is apparent that a very good temporal consistency is achieved between the GLASS and MODIS LAI values over the Zhangbei site. During the growing seasons, the LAI values of these LAI products in 2009 are significantly lower than those in other years, and the GEOV2 LAI values are generally smaller than the GLASS and MODIS LAI values at this site. For SouthWest sites, the MODIS LAI profile exhibits obviously abnormal values during the growing seasons. The GLASS, MODIS and GEOV2 LAI profiles are in good agreement during the non-growing seasons. Moreover, the temporal profiles of the GLASS, MODIS and GEOV2 LAI values show small interannual variations.

The temporal LAI profiles at the Turco and Mayo sites with the shrub biome type are displayed in Figure 7(g, h), respectively. For the Turco site, if abnormal values of the MODIS LAI product are ignored, the LAI values of these products are all less than 0.5 LAI units. The profiles of the GLASS and GEOV2 LAI products exhibit limited seasonality at this site. Nevertheless, the MODIS LAI product hardly captures seasonal and interannual variations. The GEOV2 LAI values are significantly smaller than the GLASS and MODIS LAI values before 2014. For the Mayo site, the MODIS and GEOV2 LAI temporal profiles are consistent before 2012. Moreover, the GEOV2 LAI values are systemically greater than the MODIS LAI values for these years.

Figure 7(i, j) presents the LAI temporal trajectories of evergreen broadleaf forest sites. For the Counami site, the MODIS LAI profile shows dramatic fluctuations and contains many missing values. The GEOV2 LAI values are systemically larger than the GLASS LAI values from 2002 to 2018. Moreover, the LAI values of the GEOV2 LAI product before and after 2014 are obviously inconsistent. The GEOV2 LAI values after 2014 are systemically higher than those before 2014. It is due to the GEOV2 LAI product before 2014 was generated from the SPOT-VGT data, and the GEOV2 LAI product from 2014 to 2018 was generated from the PROBA-V data. Compared with the MODIS and GEOV2 LAI values, the GLASS LAI values are closer to the LAI value derived from the high-resolution reference map at this site. For the Creón D'armagnac site, the GLASS, MODIS and GEOV2 LAI products capture similar seasonal properties. However, the GEOV2 LAI values are significantly larger than the GLASS and MODIS LAI values, and the GLASS LAI values are slightly larger than the MODIS LAI values during the growing seasons. Compared with the GEOV2 LAI values, the

GLASS and MODIS LAI values are closer to the LAI value derived from the high-resolution reference map at this site.

The temporal LAI profiles at the Sonian and Collelongo sites with deciduous broadleaf forest biome types are shown in Figure 7(k, l), respectively. Temporal profiles of the GLASS and GEOV2 LAI values are complete. However, some LAI values of the MODIS LAI temporal profile are missing. The GLASS, MODIS and GEOV2 LAI temporal profiles are consistent at the two sites during the non-growing seasons. However, significant differences in these products are observed at the Sonian and Collelongo sites during the growing seasons. The GEOV2 LAI values are larger than the GLASS LAI values in this period. The GLASS LAI product outperforms the other LAI products in terms of the LAI value derived from the high-resolution reference map at the Collelongo site.

The temporal LAI profiles at the Albufera site with evergreen needleleaf forest biome types are exhibited in Figure 7(m). The temporal profiles of the GLASS, MODIS and GEOV2 LAI values are complete and smooth. Moreover, the temporal profiles of these LAI products show similar seasonality. During the growing seasons, the GEOV2 and MODIS LAI values are significantly larger than the GLASS LAI values, especially in 2016 and 2017. The GLASS, MODIS and GEOV2 LAI values are in very good agreement with the LAI value derived from the high-resolution reference map at this site.

4.3. Direct validation

The LAI values derived from the high-resolution reference maps of the VALERI and IMAGINES projects are used for direct validation of the GLASS, MODIS and GEOV2 LAI products in this study. Figure 8 shows scatterplots of the LAI values of these LAI products versus the 58 LAI values derived from high-resolution reference maps.

The values of the GEOV2 LAI products exhibit obvious overestimation, especially for the high LAI values in forest biome types. This phenomenon is consistent with the result of spatiotemporal consistency analyses that the GEOV2 LAI values are higher than the GLASS and MODIS LAI values in forests, especially tropical rainforests (evergreen broadleaf forests). The scatterplot distribution of the MODIS LAI values versus the LAI values derived from high-resolution reference maps is relatively concentrated for low LAI values. However, the scatterplot distribution of the MODIS LAI values versus the LAI values derived from high-resolution reference maps is relatively dispersed for high LAI values. By contrast, the scatterplot distribution of the GLASS LAI values versus the LAI values derived from high-resolution reference maps is concentrated overall. The GLASS LAI values are in better agreement with the LAI values derived from high-resolution reference maps than are the GEOV2 and MODIS LAI values, especially for high LAI values. However, the GLASS LAI values are also a little underestimated at high LAI values.

The correlation between the GLASS LAI values and the LAI values derived from high-resolution reference maps ($R2 = 0.68$) is superior to the GEOV2 LAI product ($R2 = 0.55$) and the MODIS LAI product ($R2 = 0.47$). Simultaneously, the GLASS LAI product provides better accuracy (RMSE = 0.86) than the MODIS LAI product (RMSE = 1.22) and the GEOV2 LAI product (RMSE = 1.21).

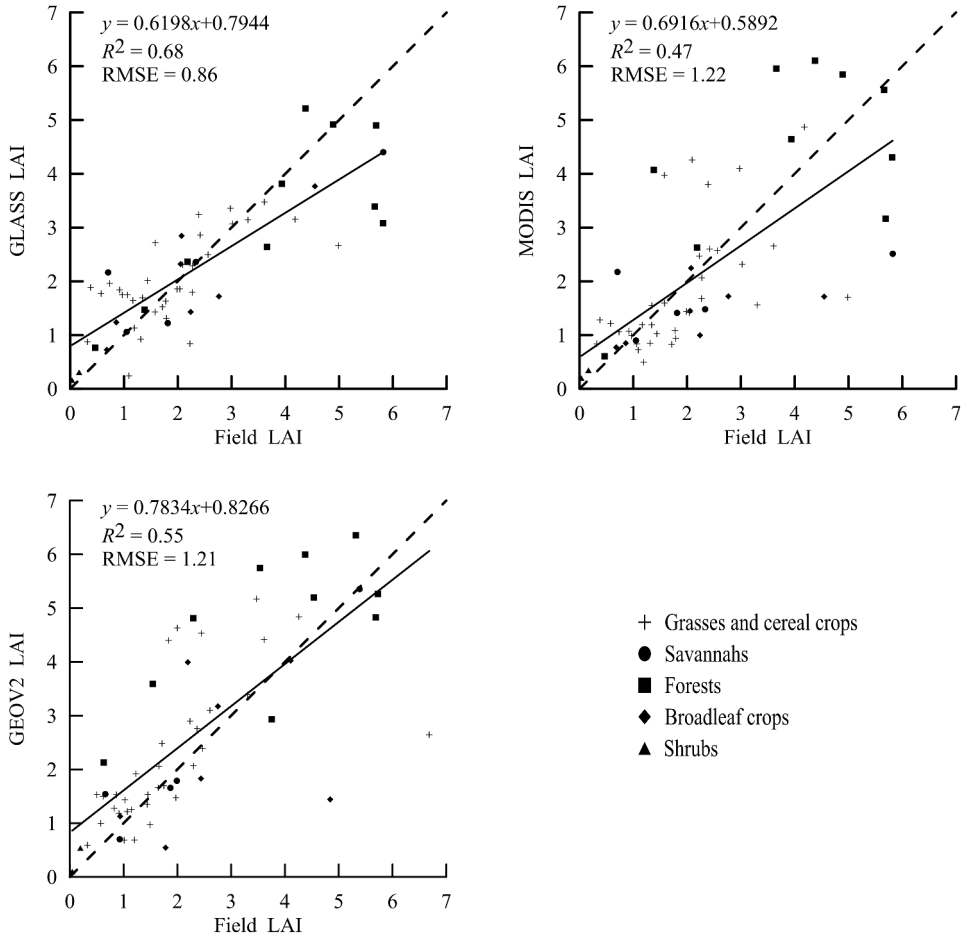

Figure 8. Scatterplots of the GLASS, MODIS and GEOV2 LAI values versus the LAI values derived from high-resolution reference maps.

5. Conclusions

The aim of this study is to evaluate the performance of the latest GLASS LAI product with a spatial resolution of 500 m. The performance of the GLASS LAI product is assessed by the inter-comparison with the latest MODIS LAI product and the GEOV2 LAI products and validation with the LAI values derived from high-resolution reference maps.

The GLASS and GEOV2 LAI products have great spatial integrity, while the MODIS LAI product contains missing pixels near the equator. These LAI products all follow the global vegetation characteristics and seasonal variability. The spatial distributions of these LAI products have slight discrepancies in savannahs, broadleaf crop, grass/cereal crop and shrub biome types. However, the spatial distribution differences of these products are obvious in forests, especially in tropical rainforests (evergreen broadleaf forests), where the GLASS LAI values are generally lower than the GEOV2 and MODIS LAI values. Differences in these LAI products are significant at the regional scale in Africa. The GLASS and GEOV2 LAI products have more continuous and realistic trajectories than

the MODIS LAI product. The MODIS temporal trajectory is noisy, particularly during the growing seasons. The LAI trajectories of these products over thirteen sites with different biome types from 2002 to 2018 show similar tendencies and interannual variations, except for evergreen broadleaf forests. Direct validation with the 58 LAI values derived from high-resolution reference maps of the VALERI and IMAGINES projects demonstrates that the accuracy of the GLASS LAI product is clearly better than that of the GEOV2 and MODIS LAI products, especially for high LAI values.

Acknowledgements

The authors would like to thank the VALERI and IMAGINES projects for providing high-spatial-resolution LAI surface maps. The authors would also like to thank the anonymous reviewers for their constructive comments that greatly helped improve the quality of this paper.

Disclosure statement

No potential conflict of interests was reported by the authors.

Funding

This work was supported in part by the National Key Research and Development Plan of China under Grant [2017YFA0603001 and 2016YFA0600103], and in part by the National Natural Science Foundation of China under Grant [41771359].

References

Bao, Y., Y. H. Gao, S. H. Lü, Q. X. Wang, S. B. Zhang, J. W. Xu, R. Q. Li, S. S. Li, D. Ma, X. H. Meng, H. Chen, and Y. Chang. 2014. "Evaluation of CMIP5 Earth System Models in Reproducing Leaf Area Index and Vegetation Cover over the Tibetan Plateau." *Journal of Meteorological Research* 28 (6): 1041–1060. doi: 10.1007/s13351-014-4023-5.

Baret, F., M. Weiss, R. Lacaze, F. Camacho, H. Makhmara, P. Pacholcyzk, and B. Smets. 2013. "GEOV1: LAI and FAPAR Essential Climate Variables and FCOVER Global Time Series Capitalizing over Existing Products. Part1: Principles of Development and Production." *Remote Sensing of Environment* 137: 299–309. doi: 10.1016/j.rse.2012.12.027.

Caixia, L., X. Wang, H. Huang, P. Gong, W. Di, and J. Jiang. 2016. "The Importance of Data Type, Laser Spot Density and Modelling Method for Vegetation Height Mapping in Continental China." *International Journal of Remote Sensing* 37 (24): 6127–6148. doi: 10.1080/01431161.2016.1252472.

Camacho, F., J. Cernicharo, R. Lacaze, F. Baret, and M. Weiss. 2013. "GEOV1: LAI, FAPAR Essential Climate Variables and FCOVER Global Time Series Capitalizing over Existing Products. Part 2: Validation and Intercomparison with Reference Products." *Remote Sensing of Environment* 137: 310–329. doi: 10.1016/j.rse.2013.02.030.

Claverie, M., J. Matthews, E. Vermote, and C. Justice. 2016. "A 30+ Year AVHRR LAI and FAPAR Climate Data Record: Algorithm Description and Validation." *Remote Sensing* 8: 3. doi: 10.3390/rs8030263.

Claverie, M., E. F. Vermote, M. Weiss, F. Baret, O. Hagolle, and V. Demarez. 2013. "Validation of Coarse Spatial Resolution LAI and FAPAR Time Series over Cropland in Southwest France." *Remote Sensing of Environment* 139: 216–230. doi: 10.1016/j.rse.2013.07.027.

Druel, A., P. Peylin, G. Krinner, P. Ciais, N. Viovy, A. Peregon, V. Bastrikov, N. Kosykh, and N. Mironycheva-Tokareva. 2017. "Towards a More Detailed Representation of High-latitude

Vegetation in the Global Land Surface Model ORCHIDEE (Orc-hl-vegv1.0)." *Geoscientific Model Development* 10 (12): 4693–4722. doi: 10.5194/gmd-10-4693-2017.

Fang, H., S. Wei, and S. Liang. 2012. "Validation of MODIS and CYCLOPES LAI Products Using Global Field Measurement Data." *Remote Sensing of Environment* 119: 43–54. doi: 10.1016/j.rse.2011.12.006.

Fang, H., Y. Zhang, S. Wei, L. Wenjuan, Y. Yongchang, T. Sun, and W. Liu. 2019. "Validation of Global Moderate Resolution Leaf Area Index (LAI) Products over Croplands in Northeastern China." *Remote Sensing of Environment*: 233. doi: 10.1016/j.rse.2019.111377.

Garrigues, S., R. Lacaze, F. Baret, J. T. Morisette, M. Weiss, J. E. Nickeson, R. Fernandes, S. Plummer, N. V. Shabanov, R. B. Myneni, Y. Knyazikhin and W. Yang. 2008. "Validation and Intercomparison of Global Leaf Area Index Products Derived from Remote Sensing Data." *Journal of Geophysical Research: Biogeosciences* 113 (G2). doi: 10.1029/2007jg000635.

Guimberteau, M., D. Zhu, F. Maignan, Y. Huang, C. Yue, S. Dantec-Nédélec, C. Ottlé, A. Jornet-Puig, A. Bastos, P. Laurent, D. Goll, S. Bowring, J. F. Chang, B. Guenet, M. Tifafi, S. S. Peng, G. Krinner, A. Ducharne, F. X. Wang, T. Wang, X. H. Wang, Y. L. Wang, Z. Yin, R. Lauerwald, E. Joetzjer, C. J. Qiu, H. Kim, and P. Ciais. 2018. ORCHIDEE-MICT (V8.4.1), a Land Surface Model for the High Latitudes: Model Description and Validation. *Geoscientific Model Development* 11 (1): 121–163. doi: 10.5194/gmd-11-121-2018.

Jin, H., A. Li, J.Bian, X. Nan, W. Zhao, Z. Zhang, and G.Yin. 2017. "Intercomparison and Validation of MODIS and GLASS Leaf Area Index (LAI) Products over Mountain Areas: A Case Study in Southwestern China." *International Journal of Applied Earth Observation and Geoinformation* 55: 52–67.doi: 10.1016/j.jag.2016.10.008.

Huang, H., C. Liu, G. S. Xiaoyi Wang, Y. C. Biging, J. Yang, and P. Gong. 2017. "Mapping Vegetation Heights in China Using Slope Correction ICESat Data, SRTM, MODIS-derived and Climate Data." *ISPRS Journal of Photogrammetry and Remote Sensing* 129: 189–199. doi: 10.1016/j.isprsjprs.2017.04.020.

Huang, Y., S. Gerber, T. Huang, and J. W. Lichstein. 2016. "Evaluating the Drought Response of CMIP5 Models Using Global Gross Primary Productivity, Leaf Area, Precipitation, and Soil Moisture Data." *Global Biogeochemical Cycles* 30 (12): 1827–1846. doi: 10.1002/2016gb005480.

Chen, J.M., and T. A. Black. 1992. "Defining Leaf Area Index for Non-flat Leaves." *Plant Cell & Environment* 15 (4): 421–429. doi: 10.1111/j.1365-3040.1992.tb00992.x.

Jiapaer, G., S. Liang, Q. Yi, and J. Liu. 2015. "Vegetation Dynamics and Responses to Recent Climate Change in Xinjiang Using Leaf Area Index as an Indicator." *Ecological Indicators* 58: 64–76. doi: 10.1016/j.ecolind.2015.05.036.

Jie, C., S. Liang, W. Verhoef, L. Shi, and Q. Liu. 2016. "Estimating the Hemispherical Broadband Longwave Emissivity of Global Vegetated Surfaces Using a Radiative Transfer Model." *IEEE Transactions on Geoscience and Remote Sensing* 54 (2): 905–917. doi: 10.1109/TGRS.2015.24695.

Liu, Z., Q. Shao, and J. Liu. 2015. "The Performances of MODIS-GPP and -ET Products in China and Their Sensitivity to Input Data (FPAR/LAI)." *Remote Sensing* 7 (1): 135–152. doi: 10.3390/rs70100135.

Meng, X., J. Cheng, and S. Liang. 2017. "Estimating Land Surface Temperature from Feng Yun-3C/MERSI Data Using a New Land Surface Emissivity Scheme." *Remote Sensing* 9: 12. doi: 10.3390/rs9121247.

Myneni, R. B., S. Hoffman, Y. Knyazikhin, J. L. Privette, J. Glassy, Y. Tian, Y. Wang, X. Song, Y. Zhang, G. R. Smith, A. Lotsch, M. Friedl, J. T. Morisette, P. Votava, R. R. Nemani, and S. W. Running. 2002. Global Products of Vegetation Leaf Area and Fraction Absorbed PAR from Year One of MODIS Data. *Remote Sensing of Environment* 83 (1–2): 214–231. doi: 10.1016/s0034-4257(02)00074-3.

Pisek, J., and J. M. Chen. 2007. "Comparison and Validation of MODIS and VEGETATION Global LAI Products over Four BigFoot Sites in North America." *Remote Sensing of Environment* 109 (1): 81–94. doi: 10.1016/j.rse.2006.12.004.

Slessarev, E. W., Y. Lin, N. L. Bingham, J. E. Johnson, Y. Dai, J. P. Schimel, and O. A. Chadwick. 2016. "Water Balance Creates a Threshold in Soil pH at the Global Scale." *Nature* 540 (7634): 567–569. doi: 10.1038/nature20139.

Song, W., M. Xihan, G. Ruan, Z. Gao, L. Linyuan, and G. Yan. 2017. "Estimating Fractional Vegetation Cover and the Vegetation Index of Bare Soil and Highly Dense Vegetation with a Physically Based Method." *International Journal of Applied Earth Observation and Geoinformation* 58: 168–176. doi: 10.1016/j.jag.2017.01.015.

Sun, Y., D. Wendi, D. E. Kim, and S.-Y. Liong. 2016. "Development and Application of an Integrated Hydrological Model for Singapore Freshwater Swamp Forest." *Procedia Engineering* 154: 1002–1009. doi: 10.1016/j.proeng.2016.07.589.

Tesemma, Z. K., Y. Wei, M. C. Peel, and A. W. Western. 2015. "The Effect of Year-to-year Variability of Leaf Area Index on Variable Infiltration Capacity Model Performance and Simulation of Runoff." *Advances in Water Resources* 83: 310–322. doi: 10.1016/j.advwatres.2015.07.002.

Tian, X., C. van der Tol, Z. B. Su,, Z. Y. Li, E. Chen, X. Li, M. Yan, X. L. Chen, X. F. Wang, X. D. Pan, F. L. Ling, C. M. Li, W. W. Fan, and L. H. Li. 2015. Simulation of Forest Evapotranspiration Using Time-Series Parameterization of the Surface Energy Balance System (SEBS) over the Qilian Mountains. *Remote Sensing* 7 (12): 15822–15843. doi: 10.3390/rs71215806.

Tian, X., M. Yan, C. van der Tol, Z. Y. Li, Z. B. Su, E. Chen, X. Li, L. H. Li, X. F. Wang, X. D. Pan, L. S. Gao, and Z. T. Han. 2017. "Modeling Forest Above-ground Biomass Dynamics Using Multi-source Data and Incorporated Models: A Case Study over the Qilian Mountains." *Agricultural and Forest Meteorology* 246: 1–14.doi: 10.1016/j.agrformet.2017.05.026.

Verger, A., F. Baret, and M. Weiss 2013. "GEOV2/VGT: Near Real Time Estimation of Global Biophysical Variables from VEGETATION-P Data." *International Workshop on the Analysis of Multi-temporal Remote Sensing Images IEEE*. doi: 10.1109/Multi-Temp.2013.6866023.

Verger, A., F. Baret, and M. Weiss. 2014. "Near Real-Time Vegetation Monitoring at Global Scale." *IEEE Journal of Selected Topics in Applied Earth Observations and Remote Sensing* 7 (8): 3473–3481. doi: 10.1109/jstars.2014.2328632.

Wang, J., J. Wang, H. Zhou, and Z. Xiao. 2017. "Detecting Forest Disturbance in Northeast China from GLASS LAI Time Series Data Using a Dynamic Model." *Remote Sensing* 9: 12. doi: 10.3390/rs9121293.

Yang, W., B. Tian, D. Huang, M. Rautiainen, N. V. Shabanov, Y. Wang, J. L. Privette, K.F. Huemmrich, R. Fensholt, I. Sandholt, D.E. Ahl, S.T.Gower, R.R. Nemani, Y. Knyazikhin, and R.B. Myneni. 2006. "MODIS Leaf Area Index Products: From Validation to Algorithm Improvement." *IEEE Transactions on Geoscience and Remote Sensing* 44 (7): 1885–1898. doi: 10.1109/tgrs.2006.871215.

Xiao, Z., S. Liang, and B. Jiang. 2017. "Evaluation of Four Long Time-series Global Leaf Area Index Products." *Agricultural and Forest Meteorology* 246: 218–230. doi: 10.1016/j.agrformet.2017.06.016.

Xiao, Z., S. Liang, R. Sun, J. Wang, and B. Jiang. 2015. "Estimating the Fraction of Absorbed Photosynthetically Active Radiation from the MODIS Data Based GLASS Leaf Area Index Product." *Remote Sensing of Environment* 171: 105–117. doi: 10.1016/j.rse.2015.10.016.

Xiao, Z., S. Liang, J. Wang, P. Chen, X. Yin, L. Zhang, and J. Song. 2014. "Use of General Regression Neural Networks for Generating the GLASS Leaf Area Index Product from Time-Series MODIS Surface Reflectance." *IEEE Transactions on Geoscience and Remote Sensing* 52 (1): 209–223. doi: 10.1109/tgrs.2013.2237780.

Xiao, Z., S. Liang, J. Wang, Y. Xiang, X. Zhao, and J. Song. 2016a. "Long-Time-Series Global Land Surface Satellite Leaf Area Index Product Derived from MODIS and AVHRR Surface Reflectance." *IEEE Transactions on Geoscience and Remote Sensing* 54 (9): 5301–5318. doi: 10.1109/tgrs.2016.2560522.

Xiao, Z., S. Liang, T. Wang, and B. Jiang. 2016b. "Retrieval of Leaf Area Index (LAI) and Fraction of Absorbed Photosynthetically Active Radiation (FAPAR) from VIIRS Time-Series Data." *Remote Sensing* 8 (4). doi: 10.3390/rs8040351.

Xiao, Z., T. Wang, S. Liang, and R. Sun. 2016c. "Estimating the Fractional Vegetation Cover from GLASS Leaf Area Index Product." *Remote Sensing* 8: 4. doi: 10.3390/rs8040337.

Yan, K., T. Park, G. Yan, C. Chen, B. Yang, Z. Liu, R. Nemani, Y. Knyazikhin, and R. Myneni. 2016a. "Evaluation of MODIS LAI/FPAR Product Collection 6. Part 1: Consistency and Improvements." *Remote Sensing* 8: 5. doi: 10.3390/rs8050359.

Yan, K., T. Park, G. Yan, Z. Liu, B. Yang, C. Chen, R. Nemani, Y. Knyazikhin, and R.B. Myneni. 2016b. "Evaluation of MODIS LAI/FPAR Product Collection 6. Part 2: Validation and Intercomparison." *Remote Sensing* 8: 6. doi: 10.3390/rs8060460.

Yan, M., X. Tian, L. Zengyuan, E. Chen, L. Chunmei, and W. Fan. 2016c. "A Long-term Simulation of Forest Carbon Fluxes over the Qilian Mountains." *International Journal of Applied Earth Observation and Geoinformation* 52: 515–526. doi: 10.1016/j.jag.2016.07.009.

Yang, J., H. Chen, N. Borjigin, M. Zhao, Y. Zhou, and Y. Huang. 2017. "Validation of the MODIS LAI Product in Qinghai Lake Basin Combined with Field Measurements Using Landsat 8 OLI Data." *Acta Ecologica Sinica* 37 (5): 322–331. doi: 10.1016/j.chnaes.2017.09.004.

Zhao, K., and S. Popescu. 2009. "Lidar-based Mapping of Leaf Area Index and Its Use for Validating GLOBCARBON Satellite LAI Product in a Temperate Forest of the Southern USA." *Remote Sensing of Environment* 113 (8): 1628–1645. doi: 10.1016/j.rse.2009.03.006.

Zhu, Z., B. Jian, Y. Pan, S. Ganguly, A. Anav, X. Liang, A. Samanta, S. Piao, R. Nemani, and R.B. Myneni. 2013. "Global Data Sets of Vegetation Leaf Area Index (Lai)3g and Fraction of Photosynthetically Active Radiation (Fpar)3g Derived from Global Inventory Modeling and Mapping Studies (GIMMS) Normalized Difference Vegetation Index (Ndvi3g) for the Period 1981 to 2011." *Remote Sensing* 5 (2): 927–948. doi: 10.3390/rs5020927.

Zhu, Z., S. Piao, R. B. Myneni, M. Huang, Z. Zeng, J. G. Canadell, P. Ciais, S. Sitch, P. Friedlingstein, A. Arneth, C. Cao, L. Cheng, E. Kato, C. Koven, Y. Li, X. Lian, Y. Liu, R. Liu, J. Mao, Y. Pan, S. Peng, J. Peñuelas, B. Poulter, T. A. M. Pugh, B. D. Stocker, N. Viovy, X. Wang, Y. Wang, Z. Xiao, H. Yang, S. Zaehle, and N. Zeng. 2016. "Greening of the Earth and Its Drivers." *Nature Climate Change* 6 (8): 791–795. doi: 10.1038/nclimate3004.